

Article

A Tunable CW Orange Laser Based on a Cascaded MgO:PPLN Single-Pass Sum-Frequency Generation Module

Dismas K. Choge ^{1,2} , Huai-Xi Chen ¹, Bao-Lu Tian ¹, Yi-Bin Xu ¹, Guang-Wei Li ¹
and Wan-Guo Liang ^{1,*}

¹ Fujian Institute of Research on the Structure of Matter, Chinese Academy of Sciences, Fuzhou 350002, China; dchoge@uoeld.ac.ke (D.K.C.); hxchen@fjirsm.ac.cn (H.-X.C.); tianbaolu1992@163.com (B.-L.T.); xuyibin@fjirsm.ac.cn (Y.-B.X.); gwli@fjirsm.ac.cn (G.-W.L.)

² University of Chinese Academy of Sciences, Beijing 100049, China

* Correspondence: wgl@fjirsm.ac.cn; Tel.: +86-0591-8371-8125

Received: 27 January 2018; Accepted: 8 March 2018; Published: 15 March 2018

Abstract: We report an all-solid-state continuous wave (CW) tunable orange laser based on cascaded single-pass sum-frequency generation with fundamental wavelengths at 1545.7 and 975.2 nm using two quasi-phase-matched (QPM) MgO-doped periodically poled lithium niobate (MgO:PPLN) crystals. Up to 10 mW of orange laser is generated in the cascaded module corresponding to a 10.4%/W nonlinear conversion efficiency. The orange output showed a temperature tuning rate of ~ 0.05 nm/ $^{\circ}$ C, and the beam quality (M^2) value of the orange laser was about 2.0. We use this technique to combine the high efficiency offered by uniformly poled crystals and the broad input wavelength acceptance characteristic of step-chirped structures.

Keywords: lithium niobate; sum frequency generation; quasi phase-matching; lasers

1. Introduction

Orange lasers with wavelengths near ~ 600 nm play an important role in a number of scientific applications such as photodynamic therapy [1], flow cytometry for excitation of fluorescent probes of 595 nm excitation wavelength [2], spectroscopy [3], astronomy [4], optogenetics and neuroscience [5], and laser projection displays [6]. So far, however, there have been no available conventional diode lasers in this spectral region due to a lack of suitable direct band gap materials [7]. Therefore, compact, stable, and efficient all-solid-state laser sources generated by nonlinear effects have gained popularity over the past thirty years with a view of overcoming this limitation. The abilities of sum frequency generation (SFG) to efficiently mix two fundamental wavelengths to generate a third wavelength is a potential technique to attain such new wavelengths with periodically poled ferroelectric crystals [8]. On the other hand, the quasi phase-matching (QPM) technique using periodically poled lithium niobate (PPLN) is quite attractive for implementing broadband SFG owing to its wide optical transparency window (350–5000 nm), a large nonlinear coefficient (d_{33}), a flexible design, and a high conversion efficiency [9]. However, reaching high efficiencies in broadband wavelength conversion remains a challenge. Nevertheless, in order to increase the input wavelength acceptance range and achieve the high efficiency of a QPM process, complementary properties of uniform poled and step-chirped crystals in a cascaded configuration can be exploited as proposed herein. The pump and signal lasers are focused into the first crystal and the generated sum frequency light co-propagates in the second crystal in which the pump and the signal are re-focused. In both crystals, SFG occurs separately, increasing the total output power and, consequently, improving the overall conversion efficiency.

Previous studies demonstrating the generation of continuous wave (CW) coherent light using cascaded crystals have been reported. For instance, a two-crystal cascade to generate 491 nm and

429 nm light with conversion efficiencies of 2.4%/W and 3.1%/W respectively in KNbO₃ crystals was demonstrated [10]. Up to 13 W of green light at 532 nm with 5%/W conversion efficiency based on two-crystal cascade PPLT crystals has also been reported [11]. Using two PPLN crystals, 780 nm second harmonic generation has been achieved with 5.6%/W conversion efficiency. Recently, 5.5 W SFG of green light was demonstrated in a two-crystal cascade of PPLN and PPLT crystals with a 50% conversion efficiency of the total fundamental power [12]. In the orange spectral region, a tunable orange laser from 601 nm to 604 nm range was successfully generated by tuning the temperature of quasi-periodically poled lithium tantalate (LT) superlattice from 150 to 195 °C, yielding a maximum output of 310 mW [13]. Up to 23 mW of narrow-line 593 nm light via intracavity SFG of a CW dual-wavelength Nd:YVO₄ laser has also been demonstrated using two volume Bragg gratings in a three-mirror cavity configuration with a temperature tunability of ~5 pm/°C [14]. Recently, also, more than 1 W all-solid state optical parametric oscillator (OPO) in the spectral range from 605 to 616 nm based on MgO:PPLN with different poling sections was reported [15]. In this scheme, tuning was achieved by varying the crystal position, temperature and etalon tilt angle. Whilst various schemes of generating visible light in the 600 nm spectral range have been extensively studied, no work has been reported on high efficiency, tunable wavelength conversion by cascaded nonlinear crystals in this range.

Here, we report the generation of all-solid state, efficient, tunable orange light by single-pass sum frequency mixing of ~1545.7 nm and ~975.2 nm laser sources in two cascaded MgO:PPLN bulk crystals. The proposed configuration offers the advantage of combining desirable solid-state properties such as the tunability of pump lasers in the 1527–1565 nm range, the high output power of ~980 nm signal laser module, high conversion efficiency offered by uniformly poled QPM crystal and wide input wavelength acceptance range due to a step-chirped (SC-PPLN) crystal. If, for instance, a broadband laser source is used rather than a narrow band highly coherent source for wavelength mixing, multiple wavelengths can be generated simultaneously in SC-PPLN. Up to 7.1 mW SFG output power was detected for the 50 mm PPLN crystal, 4.3 mW for the 20 mm SC-PPLN crystal, and 10 mW for the cascaded module corresponding to 7.4%/W, 4.5%/W, and 10.4%/W nonlinear conversion efficiencies of the total input power of the fundamental lasers, respectively. To the best of our knowledge, no work has been reported on the generation of an orange laser using MgO:PPLN bulk crystal in terms of cascaded single-pass sum frequency mixing of uniformly poled and SC-PPLN crystals, which has the advantage of tunability and high conversion efficiency.

2. Theoretical Considerations

For two fundamental lasers with input powers P_1 and P_2 incident on a nonlinear crystal of length L , the theoretical sum frequency output power can be estimated using the relation

$$P_{SFG} = \frac{32\pi^2 d_{eff}^2 P_1 P_2 L}{n_{SFG} \varepsilon_0 \lambda_{SFG}^2 c (n_1 \lambda_1 + n_2 \lambda_2)} \quad (1)$$

and the corresponding conversion efficiency can be given as

$$\eta = \frac{P_{SFG}}{P_1 P_2} \quad (2)$$

where c is the speed of light in vacuum, ε_0 is the permittivity in vacuum, and $d_{eff} = 2d_{33}/\pi$ ($d_{33} = 27.2$ pm/V) is the effective nonlinear coefficient of MgO:PPLN [16]. n_{SFG} , n_1 , and n_2 are refractive indices at λ_{SFG} , λ_1 , and λ_2 , respectively. For the cascaded module, the expected conversion efficiency for two crystals can be shown as

$$\eta_{C1+C2} = (\sqrt{\eta_{C1}} + \sqrt{\eta_{C2}})^2 \quad (3)$$

where η_{C1} and η_{C2} are the nonlinear efficiencies measured individually for Crystals 1 and 2, respectively, which follows from the superposition principle as detailed in [17].

3. Experimental Setup

The setup used in our experiment for cascaded MgO:PPLN single-pass sum-frequency generation is shown in Figure 1. The output of wavelength division multiplexer (WDM) tunable laser source (TLS) with a linewidth of <100 kHz (FWHM) in the C-band (1527–1565 nm) is amplified using an erbium-doped fiber amplifier (EDFA). It is combined with a ~980 nm module diode laser (RMS centre wavelength 973.9 nm and 0.20 nm spectral width) by a 980/1550 nm wavelength division multiplexer (WDM) with 0.26 and 0.28 dB insertion losses at 980 nm and 1550 nm respectively. The output from the single mode fiber (SMF) that is terminated with a collimator is passed through the first nonlinear uniformly poled MgO:PPLN crystal. The two overlapped input beams are focused into the first crystal and the SFG of the first crystal together with the input beams are re-focused into the second SC-PPLN nonlinear crystal with a 125 mm focal length plano-convex lenses.

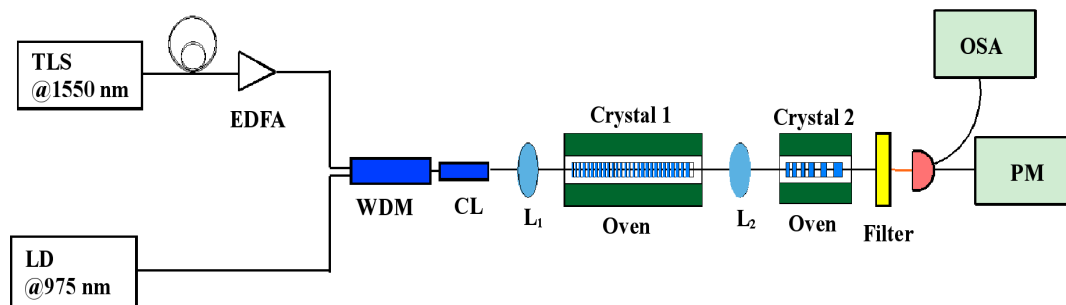


Figure 1. Schematic of the experimental setup. The beams are focused into single-pass cascaded module to generate orange output by sum frequency generation (SFG). EDFA: erbium-doped fiber amplifier; WDM: wave division multiplexer; CL: collimator; L_1 and L_2 : lenses; PM: power meter; OSA: optical spectrum analyzer; TLS, tunable laser source; LD, laser diode.

Here, the period of the first MgO:PPLN crystal is $10.3 \mu\text{m}$ and the length is 50 mm. The second MgO:PPLN crystal is a step-chirped structure with poling periods from 10.1 to $10.5 \mu\text{m}$ with a precision of $0.1 \mu\text{m}$ increase and the length is 20 mm with five equal sections. The SFG phase-matching wavelength for Crystal 1 is 1544.9 nm , while Crystal 2 showed two phase matching wavelengths at 1545.7 nm and 1556.6 nm . Both crystals were temperature-stabilized close to $31 \text{ }^\circ\text{C}$ and $25 \text{ }^\circ\text{C}$ for QPM, respectively. The output power and spectra of the up-converted orange output beam after an optical filter was measured using a laser power meter (PM100D, Thorlabs, Newton, NJ, USA) and a fiber spectrometer (BIM-6001, Brolight, Hangzhou, China) with a resolution of $0.35\text{--}1 \text{ nm}$, respectively, whereas the M^2 factor was measured using knife-edge method with Beamgage (Ophir-Spiricon, Inc., Jerusalem, Israel) laser beam analyzer.

4. Results and Discussion

4.1. Power Dependence

The maximum input fundamental powers were measured before Crystal 1 to be 418 mW (P_1) at 1545.7 nm (λ_1) and 229 mW (P_2) at 975.2 nm (λ_2). We estimated the beam waist radii of λ_1 and λ_2 to be $\sim 68 \mu\text{m}$ and $\sim 43 \mu\text{m}$ inside the crystals, respectively. A comparison of the resulting maximum output powers and corresponding conversion efficiencies with expected calculated values are summarized in Table 1. Perhaps, the total orange output power can be enhanced by anti-reflection (AR) coating the end faces of each crystal in order to minimize Fresnel reflection losses. We can infer from Table 1 that, in comparison to single crystals, the conversion efficiency is higher in the cascaded module

although lower than the expected conversion efficiency. We attribute the losses to the relative phase offset between the fundamental and SFG beams primarily due to dispersion in air and focusing lenses. The refractive nature of the lens causes color aberration since the focusing lengths for both fundamental wavelengths are different and consequently different beam waist radii results in the second crystal. In order to optimize the conversion efficiency, these limitations can be overcome by focusing the fundamental sources separately into the second crystal. Other possible reasons for the discrepancy between experimental and calculated values may originate from uneven temperature distribution within the crystals and/or poling imperfections in the QPM structure.

Table 1. Calculated and experimental comparison of output powers and conversion efficiencies in single crystals and cascaded module.

Crystal	P_{SFG} (mW)		Conversion Efficiency (% W^{-1})	
	Calculated ^a	Experiment	Calculated ^b	Experiment
Crystal 1	38.2	7.1	39.9	7.4
Crystal 2	15.2	4.3	15.9	4.5
Cascaded module	-	10.0	23.4	10.4

^a From Equation (1). ^b From Equation (2) for Crystals 1 & 2, and Equation (3) for cascaded crystals.

Figure 2a shows the CW orange power as a function of the total input power incident on the two individual crystals and for the cascaded case. The TLS power, P_1 was fixed at 418 mW (maximum) and the LD power, P_2 was increased steadily to a maximum value of 229 mW by varying the operating current. Figure 2b shows the measured beam profiles when P_1 and P_2 were 418 mW and 229 mW, respectively. For all the cases, the SFG beam was nearly identical in the horizontal direction with $M_x^2 \sim 2.1$ at 595.9 nm, 597.3 nm, and 596.9 nm for Crystal 1, Crystal 2, and the cascaded module, respectively. In the vertical direction, we measured $M_y^2 \sim 1.9$, $M_y^2 \sim 2.0$, and $M_y^2 \sim 4.1$ for Crystal 1, Crystal 2, and the cascaded module, respectively.

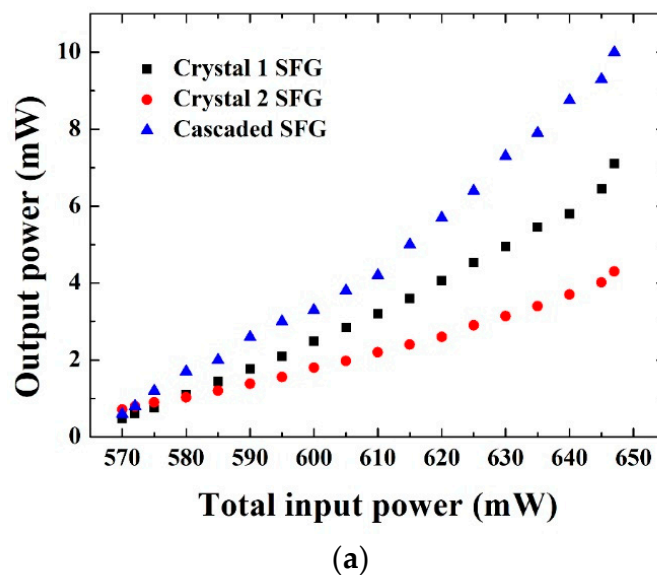


Figure 2. Cont.

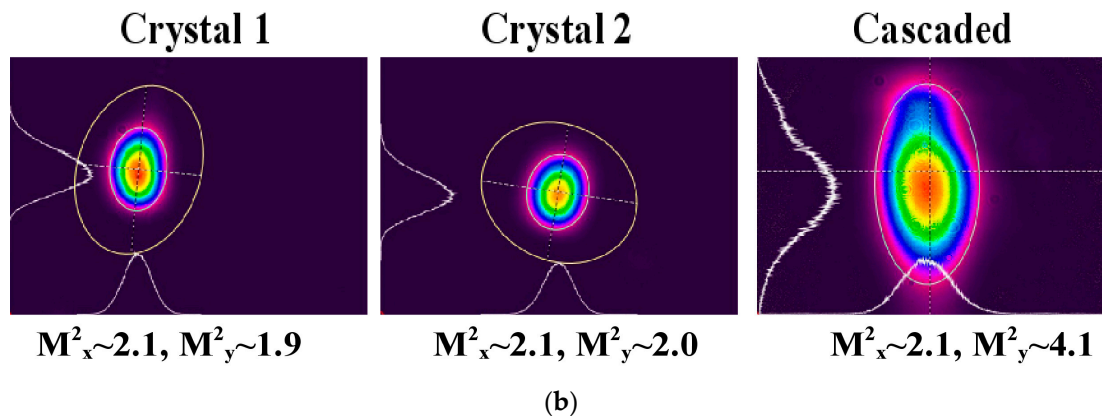


Figure 2. (a) Power of the generated orange light as a function of the total input fundamental power. (b) Beam profiles at 595.9 nm, 597.3 nm, and 596.9 nm for the three cases studied taken when P_1 and P_2 were 418 mW and 229 mW, respectively.

4.2. Output Spectra, Tunability, and Beam Stability

Figure 3 shows the normalized experimental spectra for the SFG process in Crystal 1, Crystal 2, and the cascaded module. The intensities are normalized to the maximum detection limit of our spectrometer.

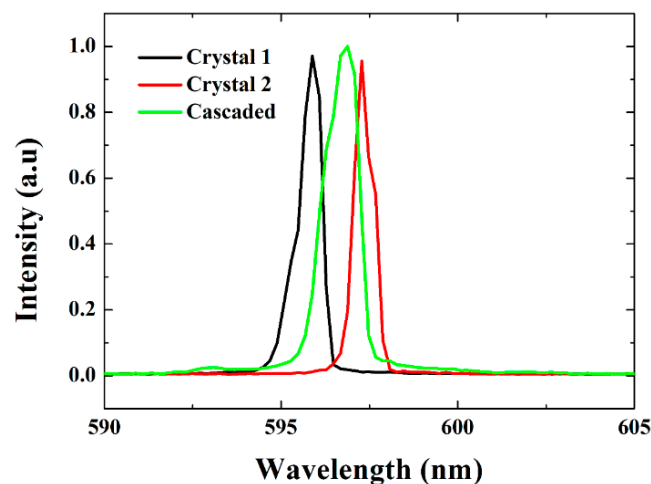


Figure 3. Normalized spectrum of the generated orange light for Crystal 1 (black), Crystal 2 (red), and the cascaded module (green).

We further established the tunability of the orange output by increasing the temperature of Crystal 1 from 25 to 90 °C, while simultaneously tuning the pump laser from 1527 to 1565 nm (upper horizontal axis) as seen in Figure 4. The corresponding output wavelengths are shown in the lower horizontal axis with a spectral resolution of ~ 0.75 nm. As the input pump wavelength was tuned, the SFG intensity exhibited oscillations as seen in Figure 5. While Crystal 1 showed a single phase matching point at 1544.9 nm, Crystal 2 revealed two phase matching points at 1545.7 nm and 1556.5 nm. The cascaded module has a broader input wavelength acceptance range compared to Crystals 1 and 2. This technique allows the pump wavelengths ranging from 1527 to ~ 1545 nm to be utilized for SFG, which is not achievable with individual crystals. It is worth noting that the orange intensity dependence on the pump wavelength shown in Figure 5 (green curve) for the cascaded case does not fit to Equation (3) as expected, from which we can conclude that the theory is not valid for this case.

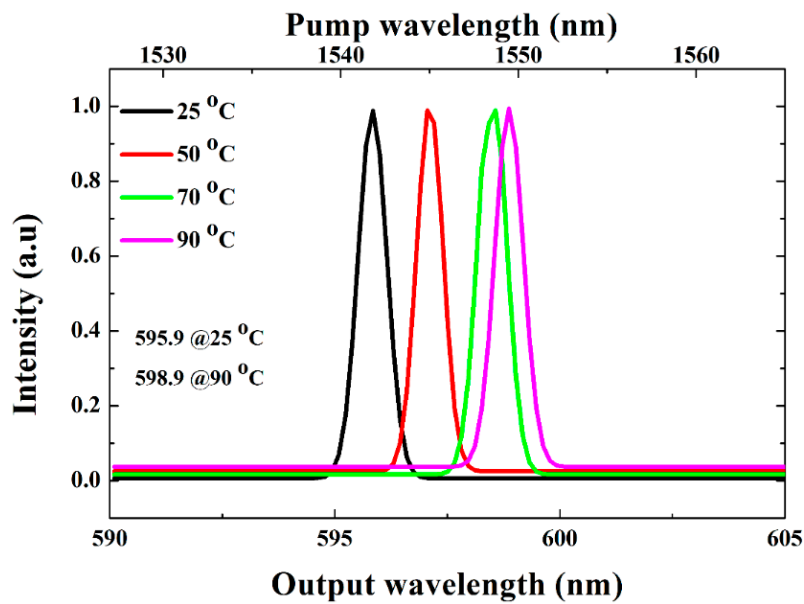


Figure 4. Spectra of orange light tuned across the 595.9–598.9 nm wavelength range.

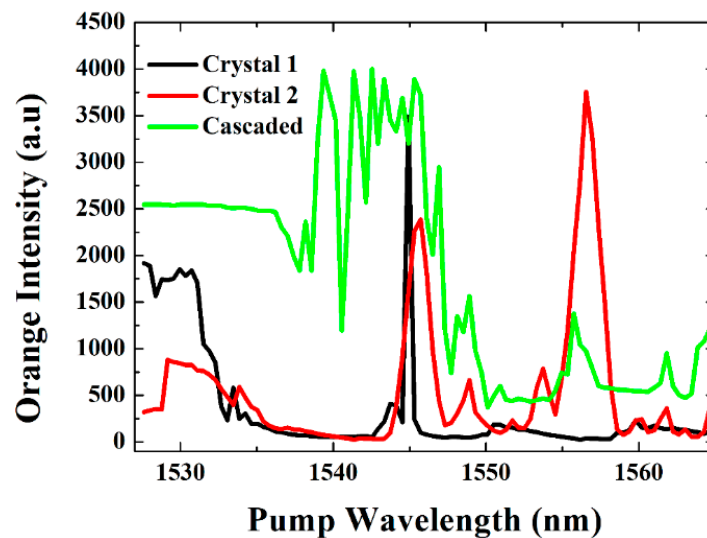


Figure 5. Measured orange laser intensity as a function of pump wavelength.

Thus, by temperature tuning, the SFG quasi phase-matching condition can be shifted owing to the fact that the refractive index of MgO:PPLN is temperature-dependent according to the Sellmeier equation. In particular, the phase-matching condition shifts to longer wavelengths with an increase in temperature. According to Figure 6, the orange light output as a function of crystal temperature can be tuned by $\sim 0.05 \text{ nm}/^\circ\text{C}$ without affecting the SFG conversion efficiency for the PPLN crystal used in this work. We therefore benefit from a temperature-assisted tunable orange light source.

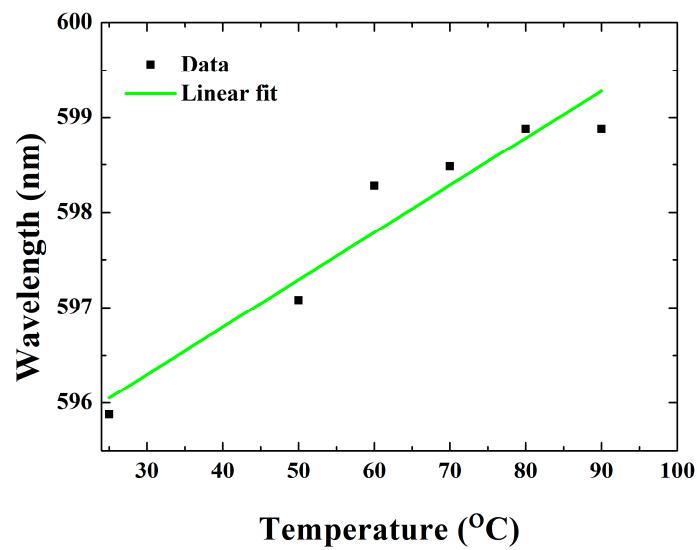


Figure 6. Variation of the generated orange light as a function of temperature tuning.

In addition, the stability of the orange light output generated by the cascaded module for one hour was measured using a power meter, showing <2.5% fluctuation of the output power around an average of 10 mW (Figure 7). We attribute this fluctuation to the stability of both fundamental lasers.

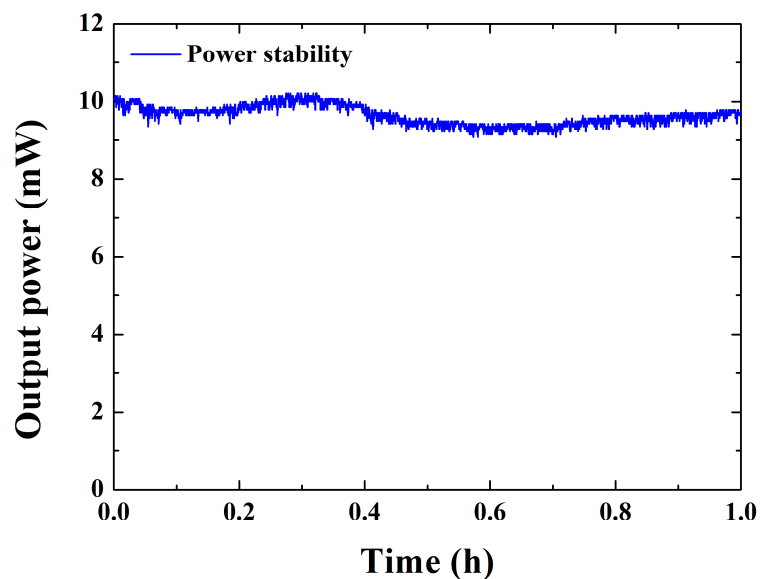


Figure 7. Stability of generated orange light with time at 596.88 nm.

5. Conclusions

We have demonstrated an all-solid-state CW broadband orange laser by cascaded single-pass sum-frequency generation with fundamental wavelengths at 1545.7 nm and ~975.1 nm. Up to 7.1 mW orange output power was detected for the 50 mm PPLN crystal, 4.3 mW for the 20 mm SC-PPLN crystal, and 10 mW for the cascaded module corresponding to 7.4%/W, 4.5%/W, and 10.4%/W nonlinear conversion efficiencies of the total input power of the fundamental lasers, respectively. A temperature tuning rate of ~0.05 nm/°C was noted, which can be understood from the temperature dependence of the refractive index of MgO:PPLN according to the Sellmeier equation. To further improve the conversion efficiency, one will need to minimize Fresnel losses by anti-reflection coating the end faces

of the two crystals as well as increasing the fundamental powers. We use this technique to combine the high efficiency offered by uniformly poled crystals and the broad input wavelength acceptance characteristic of step-chirped structures.

Acknowledgments: The authors gratefully acknowledge Fujian Science and Technology Service Network Initiative (STSI) Project (2016T3010).

Author Contributions: Dismas K. Choge conceived, designed, and performed the experiment; Dismas K. Choge and Bao-Lu Tian analyzed the experimental results; Huai-Xi Chen designed and poled the PPLN samples used in the experiment; Yi-Bin Xu and Guang-wei Li contributed in cutting, polishing, and annealing the PPLN samples; Wan-Guo Liang contributed the PPLN chips and the equipment used for preparing samples and performing experiments.

Conflicts of Interest: The authors declare no conflict of interest.

References

1. Karrer, S.; Bäumlner, W.; Abels, C.; Hohenleutner, U.; Landthaler, M.; Szeimies, R.M. Long-pulse dye laser for photodynamic therapy: Investigations In Vitro and In Vivo. *Lasers Surg. Med.* **1999**, *25*, 51–59. [[CrossRef](#)]
2. Kapoor, V.; Subach, F.V.; Kozlov, V.G.; Grudin, A.; Verkhusha, V.V.; Telford, W.G. New lasers for flow cytometry: Filling the gaps. *Nat. Methods* **2007**, *4*, 678–679. [[CrossRef](#)]
3. Marzahl, D.-T.; Metz, P.W.; Kränkel, C.; Huber, G. Spectroscopy and laser operation of Sm³⁺-doped lithium lutetium tetrafluoride (LiLuF₄) and strontium hexaaluminate (SrAl₁₂O₁₉). *Opt. Express* **2015**, *23*, 21118–21127. [[CrossRef](#)] [[PubMed](#)]
4. Chang, W.K.; Chen, Y.H.; Chang, J.W. Pulsed orange generation optimized in a diode-pumped Nd:YVO₄ laser using monolithic dual PPLN electro-optic Q switches. *Opt. Lett.* **2010**, *35*, 2687–2689. [[CrossRef](#)] [[PubMed](#)]
5. Calu, D.J.; Kawa, A.B.; Marchant, N.J.; Navarre, B.M.; Henderson, M.J.; Chen, B.; Yau, H.-J.; Bossert, J.M.; Schoenbaum, G.; Deisseroth, K.; et al. Optogenetic inhibition of dorsal medial prefrontal cortex attenuates stress-induced reinstatement of palatable food seeking in female rats. *J. Neurosci.* **2013**, *33*, 214–226. [[CrossRef](#)] [[PubMed](#)]
6. Xu, Z.Y.; Bi, Y. Large laser projection displays utilizing all-solid-state RGB lasers. In *Light-Emitting Diode Materials and Devices*; SPIE Proceedings; John Wiley & Sons Ltd.: Hoboken, NJ, USA, 2005; Volume 5632, pp. 115–122.
7. Fedorova, K.A.; Cataluna, M.A.; Battle, P.R.; Kaleva, C.M.; Krestnikov, I.L.; Livshits, D.A.; Rafailov, E.U. Orange light generation from a PPKTP waveguide end pumped by a cw quantum-dot tunable laser diode. *Appl. Phys. B Lasers Opt.* **2011**, *103*, 41–43. [[CrossRef](#)]
8. Li, G.; Chen, Y.; Jiang, H.; Chen, X. Broadband sum-frequency generation using d₃₃ in periodically poled LiNbO₃ thin film in the telecommunications band. *Opt. Lett.* **2017**, *42*, 939–942. [[CrossRef](#)] [[PubMed](#)]
9. Lee, Y.L.; Noh, Y.; Jung, C.; Yu, T.J.; Ko, D.; Lee, J. Broadening of the second-harmonic phase-matching bandwidth in a temperature-gradient-controlled periodically poled Ti: LiNbO₃ channel waveguide. *Opt. Express* **2003**, *11*, 34–35. [[CrossRef](#)]
10. Fluck, D.; Günter, P. Efficient second-harmonic generation by lens wave-guiding in KNbO₃ crystals. *Opt. Commun.* **1998**, *147*, 305–308. [[CrossRef](#)]
11. Kumar, S.C.; Samanta, G.K.; Devi, K.; Fotoniques, I.D.C.; Park, M.T. High-efficiency, multicrystal, single-pass, continuous-wave second harmonic generation. *Opt. Express* **2011**, *19*, 11152–11169. [[CrossRef](#)] [[PubMed](#)]
12. Hansen, A.K.; Andersen, P.E.; Jensen, O.B.; Sumpf, B.; Erbert, G.; Petersen, P.M. Highly efficient single-pass sum frequency generation by cascaded nonlinear crystals. *Opt. Lett.* **2015**, *40*, 5526–5529. [[CrossRef](#)] [[PubMed](#)]
13. Pan, S.D.; Yu, X.Q.; Yan, Z.; Shen, Y.; Lv, X.J.; Zhu, S.N. Efficient generation of orange light in a quasi-periodically poled LiTaO₃ crystal. *Appl. Phys. B Lasers Opt.* **2008**, *93*, 749–752. [[CrossRef](#)]
14. Chen, Y.L.; Chen, W.W.; Du, C.E.; Chang, W.K.; Wang, J.L.; Chung, T.Y.; Chen, Y.H. Narrow-line, cw orange light generation in a diode-pumped Nd:YVO₄ laser using volume Bragg gratings. *Opt. Express* **2009**, *17*, 22578–22585. [[CrossRef](#)] [[PubMed](#)]

15. Mieth, S.; Henderson, A.; Halfmann, T. Tunable, continuous-wave optical parametric oscillator with more than 1W output power in the orange visible spectrum. *Opt. Express* **2014**, *22*, 11182–11191. [[CrossRef](#)] [[PubMed](#)]
16. Gayer, O.; Sacks, Z.; Galun, E.; Arie, A. Temperature and wavelength dependent refractive index equations for MgO-doped congruent and stoichiometric LiNbO₃. *Appl. Phys. B Lasers Opt.* **2008**, *91*, 343–348. [[CrossRef](#)]
17. Hansen, A.K.; Tawfiq, M.; Jensen, O.B.; Andersen, P.E.; Sumpf, B.; Erbert, G.; Petersen, P.M. Concept for power scaling second harmonic generation using a cascade of nonlinear crystals. *Opt. Express* **2015**, *23*, 15921–15934. [[CrossRef](#)] [[PubMed](#)]



© 2018 by the authors. Licensee MDPI, Basel, Switzerland. This article is an open access article distributed under the terms and conditions of the Creative Commons Attribution (CC BY) license (<http://creativecommons.org/licenses/by/4.0/>).